

Interconnect-Aware Logic Resynthesis for Multi-Die FPGAs

XIAOKE WANG, Ghent University, Belgium

RAVEENA RAIKAR and MARKUS REIN, Ghent University, Belgium

RUIQI CHEN, Vrije Universiteit Brussel, Belgium and Ghent University, Belgium

CHANG MENG*, Eindhoven University of Technology, The Netherlands

DIRK STROOBANDT, Ghent University, Belgium

Multi-die FPGAs enable device scaling beyond reticle limits but introduce severe interconnect overhead across die boundaries. Inter-die connections, commonly referred to as super-long lines (SLLs), incur high delay and consume scarce interposer interconnect resources, often dominating critical paths and complicating physical design. To address this, this work proposes an interconnect-aware logic resynthesis method that restructures the LUT-level netlist to reduce the number of SLLs. The resynthesis engine uses die partitioning information to apply logic substitutions, which simplifies local circuit structures and eliminates SLLs. By reducing the number of SLLs early in the design flow, prior to physical implementation, the proposed method shortens critical paths, alleviates pressure on scarce interposer interconnect resources, and improves overall physical design flexibility. We further build a tool flow for multi-die FPGAs by integrating the proposed resynthesis method with packing and placement. Experimental results on the EPFL benchmarks show that, compared with a state-of-the-art framework, the proposed method reduces the number of SLLs by up to 24.8% for a 2-die FPGA and up to 27.38% for a 3-die FPGA. On MCNC benchmarks, our tool flow achieves an average SLL reduction of 1.65% while preserving placement quality. On Koios benchmarks, where fewer removable SLLs exist, several designs still exhibit considerable inter-die edge reductions. Overall, the results confirm that reducing inter-die connections at the logic level is an effective approach for multi-die FPGAs.

CCS Concepts: • **CCS Concepts**; • **Hardware** → **Combinational synthesis**; **Partitioning and floorplanning**; **Physical synthesis**;

Additional Key Words and Phrases: Interconnect, Logic Resynthesis, Multi-die FPGAs

1 Introduction

Interposer-based multi-die integration has emerged as a practical solution to overcome the reticle size limits of lithography, enabling large systems to be implemented by partitioning designs across multiple dies [1]. This approach is now widely adopted in both *application-specific integrated circuits (ASICs)* and *field-programmable gate arrays (FPGAs)* [2, 3]. However, distributing a design across dies inevitably introduces *inter-die connections*, *i.e.*, links that cross boundaries between different dies, which are also referred to as *super-long lines (SLLs)*.

Compared to *intra-die connections* that remain within a single die, inter-die connections raise two major challenges. First, they incur significantly larger delay because the signals need to traverse long physical distances across dies through the interposer and pass through additional interface circuitry. Thus, timing paths including inter-die connections are much slower, and even a small number of such connections can noticeably increase the critical path delay. This effect is particularly profound in multi-die FPGAs, where signals can cross die boundaries only through dedicated inter-die links, making timing closure more difficult to achieve [3–5]. Second, excessive inter-die connections increase physical design complexity. Inter-die connections consume scarce die-to-die

*Corresponding author.

Authors' Contact Information: Xiaoke Wang, Ghent University, Ghent, Belgium, xiaoke.wang@ugent.be; Raveena Raikar, raveena.raikar@ugent.be; Markus Rein, markus.rein@ugent.be, Ghent University, Ghent, Belgium; Ruiqi Chen, Vrije Universiteit Brussel, Brussels, Belgium and Ghent University, Ghent, Belgium, ruiqi.chen@ugent.be; Chang Meng, Eindhoven University of Technology, Eindhoven, The Netherlands, c.meng@tue.nl; Dirk Stroobandt, Ghent University, Ghent, Belgium, dirk.stroobandt@ugent.be.

links, which constrain block placement and tighten routing constraints. Prior work on single-die FPGAs has shown that higher interconnect complexity leads to longer physical design runtime [6]. In multi-die CAD flows, this effect can be further amplified. Inter-die connections tightly couple implementations on different dies, so physical implementation decisions on one die affect others. This coupling limits independent processing of dies, reduces parallelism in the design flow, and increases overall implementation difficulty and runtime.

To address these issues, prior work has explored reducing inter-die connections for FPGAs at different stages of the CAD flow. These efforts include multi-die-aware placement [7] and co-optimization of high-level synthesis directives with floorplanning [8, 9], highlighting that inter-die delay is a critical concern across different abstraction levels. Among them, partitioning-based FPGA CAD flows reduce inter-die connections through timing-aware assignment of blocks across dies [10, 11]. Previous work integrates timing-driven partitioning into the open-source *Verilog-to-Routing* (VTR) framework [12], demonstrating improvements in critical-path delay and maximum operating frequency by discouraging cuts on timing-critical paths [13, 14].

While these methods can effectively reduce the inter-die connections, they operate on a netlist that has already been fixed by logic synthesis and technology mapping, meaning the underlying logic structure that generates the inter-die connections remains unchanged. Thus, they can only redistribute existing connections across dies, rather than re-evaluating whether inter-die connections are logically necessary. Even with high-quality partitioning, many inter-die connections may persist because partitioning does not change the circuit logic, so signals required on multiple dies must still be communicated across die boundaries. As a result, existing flows across different abstraction levels mitigate inter-die connections, rather than fundamentally reducing reliance on them from the logic level.

To overcome this limitation, we explore *logic resynthesis* as a means to directly modify the netlist connectivity at the logic level. Operating on mapped netlists, such as the *lookup table* (LUT)-level netlists commonly used in FPGA design, logic resynthesis modifies the netlist so that internal signals are computed and shared differently, using functional equivalences and don't-care conditions. Conventionally, logic resynthesis has been used to optimize area, delay, or power, while we propose to leverage it to optimize inter-die connectivity in multi-die FPGAs. This logic-level restructuring capability introduces a new optimization dimension for reducing inter-die connections at their logical origin by selectively resynthesizing Boolean logic, thereby lowering SLL utilization and mitigating interposer-induced timing degradation.

The feasibility of this approach is supported by our benchmark analysis. We observe that a large fraction of signal connectivity originates from LUT-level soft logic rather than fixed architectural hard blocks. This indicates that many inter-die connections arise from flexible logic structures that can be modified, rather than rigid block-level interfaces. Consequently, even after partitioning, a large fraction of inter-die connections remains amenable to modification through logic-level restructuring.

Building on the above insight, we propose an interconnect-aware logic resynthesis method for multi-die FPGAs. Unlike existing approaches that operate at the partitioning or physical design stages, the proposed method directly eliminates unnecessary inter-die connections at their logical origin in the LUT-level netlists. To the best of our knowledge, this is the first work that optimizes inter-die connections for multi-die FPGAs at the logic resynthesis stage. Our main contributions are summarized as follows:

- (1) We formulate interconnect-aware logic resynthesis as an optimization problem that directly targets the reduction of SLLs in multi-die FPGAs.

- (2) To solve the optimization problem, we propose an SLL-aware resynthesis technique called ResynMD. It iteratively reconstructs local logic in a LUT-level netlist to eliminate unnecessary inter-die connections, while preserving functional correctness and avoiding area increase.
- (3) We develop a multi-die FPGA CAD tool flow that integrates the proposed resynthesis technique after partitioning and before physical design, which complements existing flows.

Experimental results show that on EPFL benchmarks, compared to a state-of-the-art partitioning-based multi-die FPGA CAD flow, our method reduces the number of SLLs by up to 24.8% for 2-die and 27.38% for 3-die FPGAs. On MCNC benchmarks, our method achieves an average reduction of 3.24% in inter-die connections, while preserving overall placement quality. On Koios benchmarks, the proposed method can also reduce inter-die connections while preserving post-placement quality.

The remainder of this paper is organized as follows. Section 2 describes the preliminaries. Section 3 elaborates the proposed interconnect-aware logic resynthesis method for multi-die FPGAs. The experimental results are presented in Section 4, followed by the conclusion and future work in Section 5.

2 Preliminaries

This section reviews the architectural and algorithmic background on interconnect-aware logic resynthesis for multi-die FPGAs. We first describe the characteristics of multi-die FPGA fabrics and the resulting non-uniform interconnect landscape, highlighting the role of inter-die connections and their impact on timing and physical design. We then summarize partitioning-based multi-die FPGA CAD flows. Finally, we introduce the LUT-level network representation.

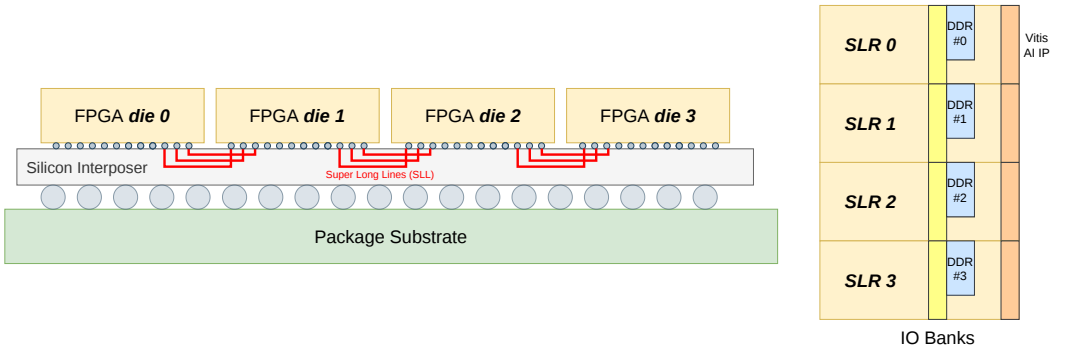


Fig. 1. Lateral and top views of a four-die FPGA system (AMD Xilinx Alveo U250 [15]).

2.1 Multi-Die FPGAs

Multi-die FPGAs integrate multiple FPGA dies within a single package, typically using a silicon interposer to provide inter-die communication. This 2.5D integration paradigm enables device scaling beyond reticle limits, but results in non-uniform interconnect characteristics between intra-die and inter-die routing resources. Signals that cross die boundaries traverse interposer links, commonly modeled as SLLs, as illustrated in Figure 1.

At the fabric level, this non-uniformity is reflected in the top-view architecture. As shown in Figure 2a, a single-die FPGA provides a largely homogeneous routing fabric. In contrast, the multi-die fabric in Figure 2b exposes inter-die communication through a limited number of fixed-location, fixed-length SLLs connected to the routing fabric via dedicated switch boxes. Compared to intra-die routing wires, SLLs offer reduced routing flexibility and distinct delay characteristics.

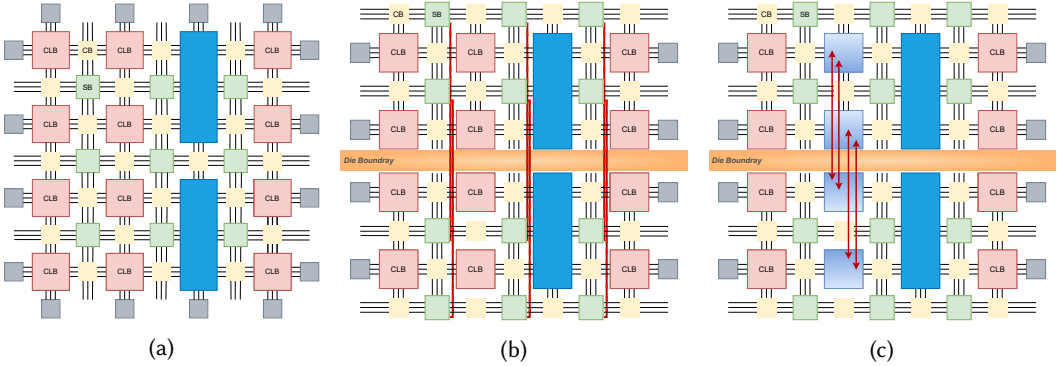


Fig. 2. Fabric-level interconnect abstractions for single-die and multi-die FPGAs: (a) a conventional single-die fabric; (b) a multi-die fabric with routing-based interposer interfaces; and (c) a multi-die fabric with tile-based interposer interfaces.

Commercial multi-die FPGAs may further employ tile-based interposer interfaces with dedicated interface tiles (e.g., Laguna columns) [16] shown in Figure 2c. Since the logic resynthesis techniques studied in this work operate on a generic logic netlist representation, they are agnostic to the specific implementation of the interposer. For clarity and compatibility with open-source academic CAD tools, we adopt the routing-based abstraction throughout this paper.

Table 1 summarizes representative delay values for intra-die routing wires and inter-die interposer links used in this work. The percentage indicates the fraction of routing tracks of each wire type within the total routing channel width. These values are derived from published technology-scaled delay models [17, 18] and serve as parameters for characterizing the timing differences between routing resources.

Table 1. Intra-die (22 nm) and inter-die (45 nm interposer) wire delays.

Wire Type	Technology	Delay (ps)	Percentage (%)
L1	22 nm (Intra-die)	76.2	50
L2	22 nm (Intra-die)	94.9	25
L6	22 nm (Intra-die)	212.0	25
L36	45 nm (Inter-die)	2223.7	48

2.2 Partitioning-Based Multi-Die FPGA Flow

By decomposing a monolithic design into multiple sub-circuits on multiple dies, partitioning reduces the optimization space of the CAD problems and enables scalable and partially parallel CAD processing, while still requiring careful coordination of inter-die connections. Figure 3 illustrates two representative partitioning-based CAD strategies for multi-die FPGA implementation, which differ in whether partitioning is performed before or after packing. In packing-first flows, LUTs are first clustered into architecture-specific blocks, such as configurable logic blocks (CLBs), and partitioning is subsequently applied to these packed blocks [2, 13]. This ordering closely reflects physical constraints and simplifies downstream placement and routing, but fixes the logic connectivity at the granularity of packed blocks. In contrast, partitioning-first flows partition the primitive netlist before packing, allowing logic connectivity to be considered before architectural constraints are

fully imposed. Several state-of-art multi-die CAD flows [2, 13, 14, 19] use the partitioning-first paradigm. The netlist is first partitioned into sub-circuits on multiple dies, after which packing, placement, and routing are performed for each die.

Our interconnect-aware resynthesis technique is better suited to the partition-first flow. In this flow, we insert logic resynthesis after partitioning and before packing. Operating on the LUT-level netlist at this stage preserves more freedom for modification because LUTs have not yet been grouped into CLBs. Compared with a CLB-level netlist, the LUT-level representation is finer-grained and exposes more connections, allowing resynthesis to restructure logic and reduce inter-die connections more effectively.

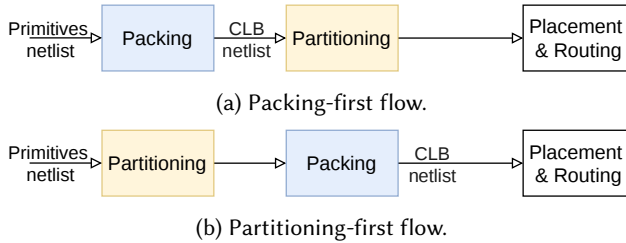


Fig. 3. Two partitioning-based CAD strategies for multi-die FPGAs: (a) a packing-first flow, where packing precedes partitioning; and (b) a partitioning-first flow, where the partitioning is performed before packing.

2.3 LUT-Level Network Representation

FPGA logic synthesis typically operates on circuits represented as graph-based logic networks, which provide a structural abstraction of Boolean functionality. After optimizing the logic networks, technology mapping transforms the circuit into a netlist of k -input LUTs. The LUT-level netlist explicitly defines the logic connectivity exposed to physical design processes, and therefore serves as the interface between logic synthesis and architecture-aware optimization. A LUT-level netlist can be viewed as a directed acyclic graph $G = (V, E)$. In this graph, each node $v \in V$ represents a k -input LUT implementing a local Boolean function f_v . Each directed edge $(u, v) \in E$ denotes a signal connection from the u to v . Operating at the LUT level enables fine-grained optimization of inter-die connectivity by directly manipulating inter-LUT signals while ensuring seamless integration with downstream CAD flows.

For a node v , its *transitive fanin (TFI)* is the set of nodes that can reach v through directed paths in G . Similarly, its *transitive fanout (TFO)* is the set of nodes reachable from v . These structural regions characterize the upstream and downstream influence of v in the logic network. The *maximum fanout-free cone (MFFC)* of node v , denoted $\text{MFFC}(v)$, is the maximal subgraph rooted at v such that every node in the subgraph has no fanout outside the subgraph. Removing v will disconnect all nodes in $\text{MFFC}(v)$ from the primary outputs. The MFFC corresponds to the portion of logic exclusively controlled by v , and removing v eliminates its entire MFFC.

3 Interconnect-Aware Resynthesis for Multi-Die FPGAs

This section presents ResynMD, an interconnect-aware logic resynthesis method for multi-die FPGAs. We first introduce the motivation and overall tool flow in Section 3.1. Then, Section 3.2 formulates the SLL-aware resynthesis problem and optimization objective. Section 3.3 describes the core components of the proposed resynthesis engine. Finally, Section 3.4 discusses the trade-off between partition imbalance and inter-die connection reduction.

3.1 Motivation and Overview

Modern applications mapped onto multi-die FPGAs typically contain large amounts of soft logic (*i.e.*, logic implemented using LUTs) with many interconnections. Compared with hard blocks such as DSPs and RAMs, soft logic is highly flexible in placement and routing and is therefore more likely to be distributed across dies. While hard blocks generally reside at fixed sites and are rarely split across dies, LUT-level logic in large designs is frequently partitioned, producing numerous cross-die connections implemented using SLLs. Because SLLs incur high delay and limited routing flexibility, they frequently dominate critical paths and contribute significantly to routing congestion.

This work focuses on reducing the number of SLLs by targeting the logic-level origins of inter-die connectivity. These inter-die connections are not purely required by architectural constraints, but often stem from the logic implementation of the mapped LUT-level netlist. Consequently, modifying the logic implementation can often replace cross-die signals with functionally equivalent in-die implementations, thereby reducing the inter-die connections. By directly restructuring the logic to reduce inter-die connections, ResynMD tool flow complements existing partitioning-first CAD flows for multi-die FPGAs [7, 14] (see Figure 3b), which optimize inter-die connections through partitioning or placement without altering the circuit at the logic level.

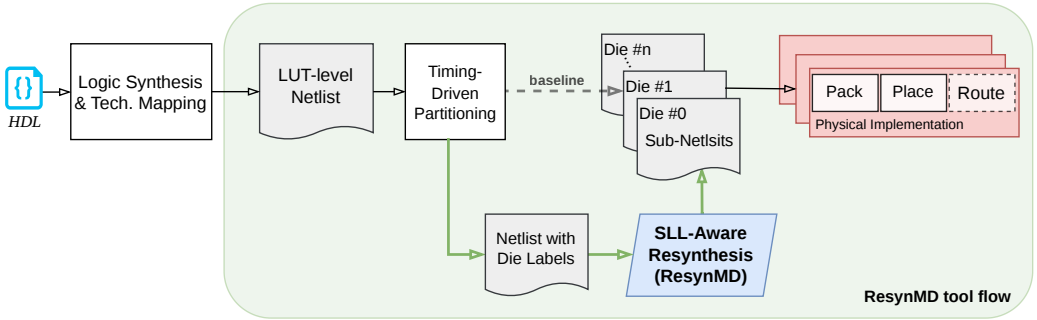


Fig. 4. The proposed ResynMD tool flow. Compared with the baseline partitioning-first CAD flows (Fig. 3b), this tool flow adds an SLL-aware resynthesis step between partitioning and physical implementation.

Figure 4 shows the ResynMD tool flow. It starts from a synthesizable HDL description and outputs a physical implementation for a multi-die FPGA. It first performs conventional logic synthesis and technology mapping to obtain a LUT-level netlist. The netlist is then partitioned across multiple dies using a timing-aware partitioner, which reduces inter-die connections on critical paths while balancing logic resources across dies. After partitioning, each LUT is assigned a fixed die label, resulting in a partition-annotated netlist in which inter-die connections correspond to nets spanning multiple dies. ResynMD, which is an SLL-aware logic resynthesis step, is then applied to this partition-annotated netlist. Its objective is to reduce the number of SLLs by restructuring netlist logic while preserving the fixed die assignments. Following resynthesis, the optimized netlist is split into per-die sub-netlists. Thereafter, the standard physical design stages, including packing, placement, and routing, are executed for each die.

Compared to the existing partitioning-first CAD flows, such as LiquidMD [14, 20, 21], the key distinction of the proposed tool flow in Figure 4 is the SLL-aware logic resynthesis step that is applied after partitioning but before physical implementation, as illustrated by the blue segment in Figure 4. To the best of our knowledge, ResynMD is the first approach that explicitly targets logic-level restructuring for reducing inter-die connections. This introduces a new optimization dimension that is complementary to existing partitioning-based and placement-based multi-die

optimization techniques and can provide synergistic benefits when integrated into current multi-die FPGA design flows. The following subsection details the problem formulation and the core components of the proposed SLL-aware resynthesis method.

3.2 Problem Formulation of SLL-Aware Logic Resynthesis

Conventional logic synthesis methods, such as [22–25], optimize metrics such as area or delay without considering the multi-die context and do not explicitly reduce inter-die connections. In contrast, the proposed SLL-aware logic resynthesis operates on a partitioned LUT-level netlist and directly targets inter-die connections. In this setting, the die assignment of each LUT is fixed by the partitioning stage, and only functionally equivalent logic transformations are permitted.

Let $G = (V, E)$ denote the LUT-level netlist with partition labels, where each node $v \in V$ is assigned to a die $D(v)$. A connection between nodes u and v is inter-die (and thus implemented using an SLL) if $D(u) \neq D(v)$. We define the *total number of SLLs* (also called *inter-die connectivity*) as

$$N_{sll}(G) = \sum_{(u,v) \in E} \mathbb{I}[D(u) \neq D(v)], \quad (1)$$

where $\mathbb{I}[\cdot]$ is an indicator function that equals 1 if the connection between u and v crosses the die boundary and 0 otherwise.

Our objective is to construct a functionally equivalent netlist $G' \equiv G$ that minimizes the number of SLLs without increasing the netlist area. Formally, the objective is

$$\min_{G' \equiv G} N_{sll}(G') \text{ subject to } Area(G') \leq Area(G), \quad (2)$$

where the function $Area(\cdot)$ measures the netlist area in terms of LUT count.

Because global optimizing Equation (2) over all equivalent netlists needs exploring a huge combinatorial search space, we adopt a greedy heuristic that iteratively applies local resubstitution [22] transformations, which preserve functionality while modifying the fanin structure of nodes. This approach offers good scalability and computational efficiency for large-scale circuits. In each iteration, a transformation is accepted only if it strictly reduces the total number of SLLs and satisfies the area constraint. More details on the resubstitution procedure are presented in Section 3.3.

3.3 Details of SLL-Aware Logic Resynthesis

3.3.1 Greedy Algorithm for SLL-Aware LUT-Level Resynthesis. This subsection presents the core algorithm of the proposed SLL-aware logic resynthesis method. The method builds upon the resynthesis technique MFS [26]. Unlike conventional MFS, which optimizes traditional metrics such as area or delay, our new contributions lie in adapting the resynthesis approach to the multi-die context with a specific focus on reducing inter-die connections, as illustrated in Figure 5. The inter-die connections are reduced by performing *LUT-level resubstitution*. Here, *resubstitution* [26, 27] refers to a local logic transformation that replaces a node with a functionally equivalent implementation expressed in terms of a selected set of other nodes (called *divisors*) in the netlist.

As shown in Algorithm 1, the input of our resynthesis procedure is a partition-annotated LUT-level netlist G , where each node is assigned a die label determined during partitioning. The output is an optimized netlist G' with fewer inter-die connections, which can be directly fed into the subsequent physical implementation stages. The algorithm initializes the working netlist G' as the input netlist G (Line 1). Then, it processes each node v in G' in topological order (Line 2), ensuring that fanin nodes are handled before their fanouts and preventing cyclic dependencies during resubstitution. We call the node v being processed the *pivot node*. For each pivot node, the algorithm first checks whether all fanins of v reside on the same die as v (Line 3). If so, node v

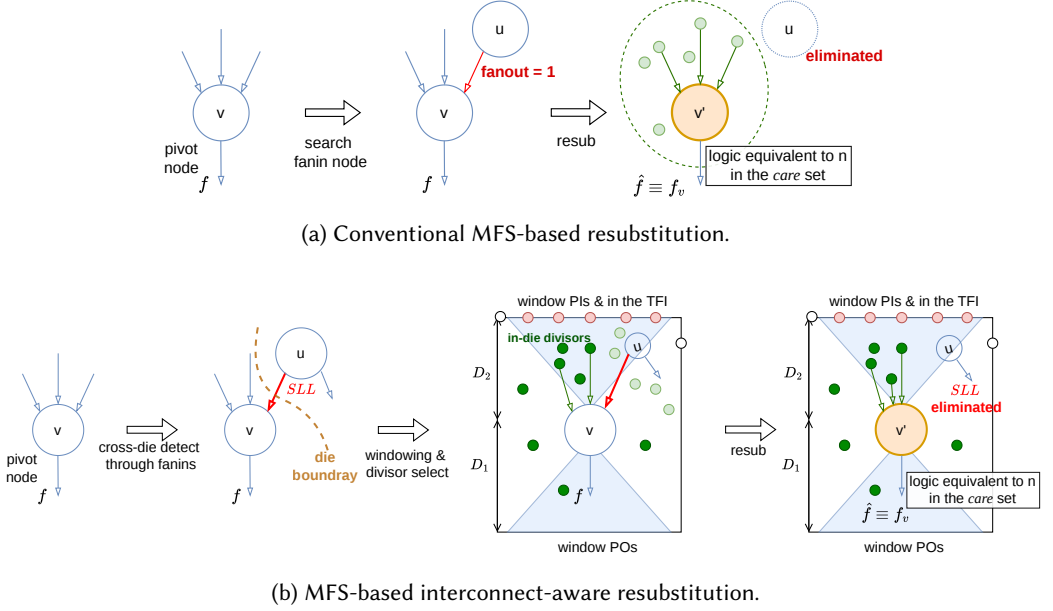


Fig. 5. Comparison between conventional MFS-based LUT-level resubstitution and the proposed interconnect-aware resubstitution.

Algorithm 1: Greedy SLL-Aware Logic Resynthesis by LUT-level Resubstitution

Input: LUT-level netlist $G = (V, E)$, die mapping $\mathcal{D}(v)$ for each node $v \in V$

Output: Optimized LUT-level netlist G' with reduced number of SLLs.

```

1 Initialize working netlist  $G' \leftarrow G$ ;
2 for each pivot node  $v$  in  $G'$  in topological order do
3   if  $\forall u \in \text{fanin}(v) : \mathcal{D}(u) = \mathcal{D}(v)$  then
4      $\lfloor$  continue; // Skip the node without cross-die fanins
5   Sub-circuit  $W(v) \leftarrow \text{BuildWindow}(G', v)$ ; // Extract local circuit surrounding  $v$ 
6   Divisor set  $\mathcal{S}_d(v) \leftarrow \text{GetSLLAwareDivisors}(W(v), v)$ ; // Get divisors used to re-express  $v$ 
7   New function  $\hat{f}_v \leftarrow \text{FindEquivFunc}(W(v), v, \mathcal{S}_d(v))$ ; // Find  $v$ 's equivalent function
8   if  $\hat{f}_v$  exists then
9     New node  $v' \leftarrow \text{LUTImplement}(\hat{f}_v)$ ;
10    if #cross-die fanins of  $v' <$  #cross-die fanins of  $v$ 
11    and  $\text{Area}(v') \leq \text{Area}(v)$  then
12       $\lfloor G' \leftarrow \text{ApplyResubstitution}(G', v, v')$ ; // Replace  $v$  with new node  $v'$ 
13 return  $G'$ ;

```

has no cross-die fanins and cannot contribute to SLL reduction, and is therefore skipped (Line 4). For node v with cross-die fanins, a local *window* $W(v)$ is constructed (Line 5). This window is a sub-circuit surrounding node v that captures the local logic context of v while limiting the scope of optimization to ensure computational tractability. Within this window, a set of SLL-aware divisors $\mathcal{S}_d(v)$ is collected (Line 6), which are potential candidate signals used to construct v 's

new implementation. These divisors consist only of nodes located on the same die as v , ensuring that any new implementation of v can be realized without introducing new cross-die fanins and enabling the elimination of existing ones. Using these divisors, the algorithm attempts to derive an equivalent Boolean function \hat{f}_v for node v (Line 7). Note that such a function may not always exist (see Section 3.3.4 for details). If no such function exists, the node v remains unchanged. Otherwise, the function \hat{f}_v is implemented using one or more LUTs to create a new node v' (Line 8), which serves as a candidate resubstitution for v . The candidate resubstitution is accepted only if the new node v' has fewer cross-die fanins than the original node v , and does not increase area in terms of LUT count (Lines 10 and 11). When both conditions are satisfied, the resubstitution is committed to the working netlist G' (Line 12), and the algorithm proceeds to the next node. After all nodes have been processed, the optimized netlist G' is returned (Line 13).

The above greedy strategy guarantees monotonic reduction of cross-die fanins of each node v in the LUT-level netlist while maintaining scalability for large designs. Since each accepted resubstitution removes at least one inter-die fanin edge of node v (Line 10), the total number of SLLs N_{sll} decreases monotonically ensuring the convergence of the procedure. Moreover, the area constraint in Equation (2) is enforced through the condition check in Line 11, which disallows any resubstitution that increases LUT count.

Algorithm 1 relies on three key procedures corresponding to three main components of the SLL-aware resynthesis method: *BuildWindow*, which constructs the local optimization region, *GetSLLAwareDivisors*, which selects same-die candidate signals, and *FindEquivFunc*, which constructs an equivalent function, typically via SAT-based resubstitution. These components are described in detail in Section 3.3.2–3.3.4.

3.3.2 Window Construction. This step corresponds to Line 5 in Algorithm 1. We adopt the same window construction strategy as MFS [26]. As illustrated in the middle of Figure 5b, for each pivot node v (i.e., node being processed for resubstitution), its window $W(v)$ is a sub-circuit surrounding v that captures the local logic context relevant for v 's resubstitution. $W(v)$ is formed by expanding its TFOs up to a limited depth D_1 . Then, D_2 levels of TFIs of the pivot node v determines the window *primary inputs* (PIs). After that, the internal nodes are obtained through a topologically ordered traversal of the induced subgraph, forming the window $W(v)$.

3.3.3 Divisor Selection. This step corresponds to the computation of the divisor set $S_d(v)$ in Line 6 of Algorithm 1, where candidate divisors are extracted from the local window $W(v)$ and filtered according to their die assignment. Divisors are signals within the local window $W(v)$ that can be used to re-express the Boolean function of the pivot node v . Their selection process is illustrated in the middle part of Figure 5b. When cross-die fanins of the pivot are detected, a local window is constructed around the pivot node. Window PIs are split according to whether they belong to the transitive fanin of the pivot. The nodes on structural paths between the pivot and its TFI-related window PIs are collected as potential divisors, excluding the pivot itself and the nodes in its maximum fanout-free cone (MFFC). Additionally, window nodes whose structural support does not depend on non-TFI window PIs are also considered. To limit complexity, divisors that exceed a predefined logic-level bound are discarded, and the total number of divisors is capped.

To incorporate inter-die interconnection awareness, each divisor is classified according to its die assignment relative to the pivot node. The divisors located on the same die (highlighted in dark green in Figure 5b) as the target are greedily selected and constitute the final in-die divisor set $S_d(v)$.

In conventional resubstitution, candidate divisors are selected solely based on functional or structural criteria without considering their physical die assignment, sometimes introducing new

inter-die connections. In contrast, the proposed approach enforces a greedy, SLL-aware divisor selection strategy that deterministically considers same-die signals. This enables the following SAT-based resubstitution approach to eliminate unnecessary inter-die connections.

3.3.4 SAT-Based Resubstitution. This step corresponds to the Line 7 of Algorithm 1. The goal is to compute a function \hat{f} that is equivalent to f_v (the function of the pivot node v), expressed using a subset of in-die divisors $S'_d \subseteq S_d(v)$. The key idea is to selectively eliminate cross-die fanins of the pivot node v by expressing its function f_v using only in-die signals. For a pivot node v , we construct its equivalent function \hat{f} in a structured manner, as summarized in Algorithm 2. Rather than searching for arbitrary divisor combinations, we restrict the construction to eliminate cross-die dependencies.

Algorithm 2: *FindEquivFunc*($W(v), v, S_d(v)$)

Input: Local window $W(v)$, pivot node v , divisor set $S_d(v)$

Output: Equivalent function \hat{f} or \emptyset (i.e., \hat{f} does not exist)

```

1 Select a cross-die fanin  $u \in \text{fanin}(v)$ ;
2  $\text{BaseDivisors} \leftarrow \text{fanin}(v) \setminus \{u\}$ ;
3  $C \leftarrow \text{ExtractCareSet}(W(v), v)$ 
4 if SATBasedExistCheck( $f_v, C, S'_d$ ) then
5    $S'_d \leftarrow \text{BaseDivisors}$ ;
6   return  $\hat{f} \leftarrow \text{Interpolate}(S'_d)$ ;
7 for each divisor  $d \in S_d(v)$  do
8    $S'_d \leftarrow \text{BaseDivisors} \cup \{d\}$ ;
9   if SATBasedExistCheck( $f_v, C, S'_d$ ) then
10    return  $\hat{f} \leftarrow \text{Interpolate}(S'_d)$ ;
11 return  $\emptyset$ ;
```

First, this procedure is triggered by identifying a cross-die fanin $u \in \text{fanin}(v)$ and attempting to remove it. The base divisor subset $S'_d = \text{BaseDivisors}$ is initialized by excluding u while retaining all remaining fanins (Line 2). If f_v can be expressed using this reduced set under the care constraint, the cross-die edge (u, v) is directly eliminated.

If this direct elimination fails, we traverse the in-die divisor set $S_d(v)$ (Line 7). For each candidate divisor d , we construct a new divisor subset S'_d by augmenting the base divisors with d , i.e., by adding a single in-die divisor to compensate for the removed cross-die dependency. Feasibility is then re-evaluated for this augmented set.

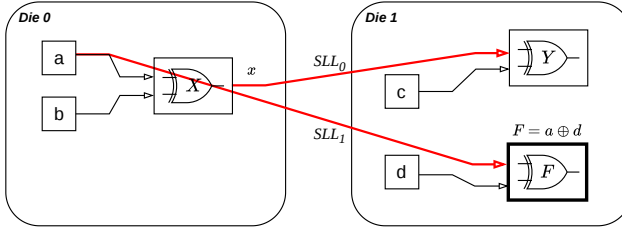
For each constructed divisors subset S'_d , a SAT-based existence check [26] is performed under the extracted care set C to determine whether f_v can be equivalently expressed using signals in S'_d . If the SAT-based existence check succeeds, an interpolation is extracted to construct the equivalent function \hat{f}_v [28]. The interpolation depends only on signals in S'_d and preserves equivalence under the care set C . The derived function \hat{f}_v is then implemented as a new LUT node v' whose fanins correspond to the selected divisors in S'_d . Node v' is inserted into the original network, and all fanout connections of the original pivot node v are redirected to v' . Subsequently, node v and any newly unreachable logic in its $\text{MFFC}(v)$ are removed from the network. This network update corresponds to line 12 in Algorithm 1.

3.3.5 Example. We use a small 2-input LUT (LUT2 in short) netlist as an example to illustrate how our SLL-aware resynthesis technique can reduce redundant inter-die connections. Note that LUT2 is used here for ease of presentation, and the proposed method is applicable to general LUT sizes.

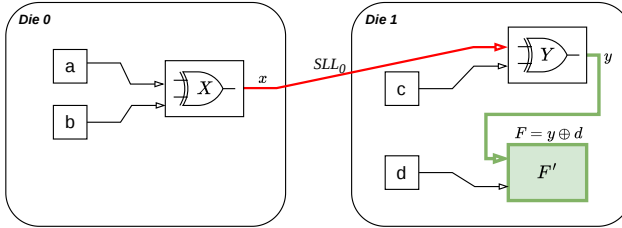
Pre-resynthesis logic. As shown in Figure 6a, consider a partitioned LUT-level netlist mapped onto a two-die FPGA. Let a, b, c, d be primary inputs. The LUT node X is placed on Die 0, while nodes Y and F are placed on Die 1. Node F is the pivot node to be resubstituted. Signal x crosses the die boundary, forming an inter-die connection between X on Die 0 and Y on Die 1. In addition, the pivot node F on Die 1 depends directly on signal a on Die 0, introducing an extra inter-die fan-in that we aim to eliminate.

The logic functions in the 2-input LUTs are defined as:

$$\begin{aligned} X &= a \oplus b \\ Y &= X \oplus c \\ F &= a \oplus d \end{aligned} \quad (3)$$



(a) Pre-resynthesis: the original LUT-level netlist before resubstitution (F is pivot node).



(b) After resynthesis: SLL-aware resubstitution eliminating the redundant inter-die dependency on a .

Fig. 6. Example of SLL-aware resynthesis.

Don't-care and care set definition. As discussed in Section 3.3.4, the functionality of a pivot node is required to be preserved only on its care set, and the don't-care cases can be exploited to enable more flexible resubstitution. For illustrative purposes, we assume that input assignments with $b \neq c$ are don't-cares of the pivot node F . In other words, we only care about the functional equivalence under the input cases when $b = c$. The don't-care and care conditions are defined as:

$$\begin{aligned} DC(a, b, c, d) &= b \oplus c, \\ C(a, b, c, d) &= \neg(b \oplus c). \end{aligned} \quad (4)$$

Resynthesis process and post-resynthesis logic. Node F is the pivot node to start the process. As the current example is simple, following the windowing method introduced in Section 3.3.2, all of the LUT nodes across two dies will be covered in the *window*. During the divisor selection step, within the resynthesis window, only the *in-die* signals are available as candidate divisors, including

Y , c and d . Exploiting the don't-care conditions in Equation (4) and the candidate divisors, we can use the method in Section 3.3.4 to construct an equivalent function of F . First, the cross-die fanin a is selected and excluded, while the remaining fanin d is extracted as *BaseDivisors*. Following Algorithm 2, two types of divisor subsets are examined. The first consists only of *BaseDivisors* (i.e., $S'_d = \{d\}$). The second augments *BaseDivisors* with an additional in-die divisor Y , resulting in $S'_d = \{d, Y\}$. The SAT-based existence check returns true for $S'_d = \{d, Y\}$, indicating that F can be equivalently expressed using only in-die divisors. The interpolated function is therefore derived as

$$F' = Y \oplus d. \quad (5)$$

As shown in Table 2, the new function F' is equivalent to F on all care minterms, which ensures the functional correctness after resubstitution. After resubstituting F by F' , the post-resynthesis netlist is shown in Figure 6b. F' no longer depends on the inter-die signal a , while the necessary inter-die dependency on X is preserved via node Y . The amount of SLLs (N_{sll}) of this small example decreases from 2 to 1.

Table 2. Truth table of the pivot node before and after resubstitution. Gray rows correspond to **don't-care** conditions ($b \neq c$). Signals Y and d are in-die divisors used to reconstruct F .

a	b	c	d	X	Y	F (orig.)	F' (new)	care?
0	0	0	0	0	0	0	0	1
0	0	0	1	0	0	1	1	1
0	0	1	0	0	1	0	1	0
0	0	1	1	0	1	1	0	0
0	1	0	0	1	1	0	1	0
0	1	0	1	1	1	1	0	0
0	1	1	0	1	0	0	0	1
0	1	1	1	1	0	1	1	1
1	0	0	0	1	1	1	1	1
1	0	0	1	1	1	0	0	1
1	0	1	0	1	0	1	0	0
1	0	1	1	1	0	0	1	0
1	1	0	0	0	0	1	0	0
1	1	0	1	0	0	0	1	0
1	1	1	0	0	1	1	1	1
1	1	1	1	0	1	0	0	1

3.4 Partition Imbalance Induced by Inter-Die Resynthesis

In addition to minimizing the number of inter-die connections, partitioning-based multi-die FPGA CAD flows are also expected to maintain a balanced distribution of logic resources across dies. Partition balance is a key feasibility constraint: a severely imbalanced die can become overutilized, leading to packing/placement failures or degraded QoR. A commonly used metric is the partition imbalance ratio, denoted by ρ , which quantifies the deviation of logic distribution from an ideal uniform partition [19]. It is defined as

$$\rho = \max_{k \in \{0, \dots, K-1\}} \left(\frac{|V_k|}{|V|/K} \right), \quad (6)$$

where K is the number of dies, $|V_k|$ denotes the number of logic nodes assigned to die k , and $|V|$ denotes the total number of logic nodes. In practice, an upper bound on ρ called UB is imposed during partitioning to ensure feasible packing and placement on each die.

Note that the proposed SLL-aware resynthesis does not strictly preserve the original partition balance. The success of resubstitution is inherently opportunistic and each success has an asymmetric and localized impact on the involved dies. Figure 5a illustrates a representative scenario. On the destination die, the pivot node v is replaced by another node v' , so the size typically remains unchanged. On the source die, the effect depends on the fanout structure. If the predecessor v has no other fanouts, both v and its MFFC become redundant and can be eliminated, thereby reducing the size of the corresponding die by one or more nodes. Otherwise, no node reduction occurs. This size reduction behaviour is the original purpose of conventional MFS and is inherited by SLL-aware resynthesis, which consequently introduces uncertainty in die imbalance. As a result, the number of logic nodes assigned to individual dies may change, leading to a variation in the observed imbalance factor ρ . Since resubstitution is applied greedily in topological order, such node removals are difficult to predict analytically. Although the total number of LUTs in the netlist is guaranteed to be non-increasing (Line 11 in Algorithm 1), the per-die logic distribution may vary slightly. Therefore, we report the imbalance factor before and after resynthesis in Sections 4.3 and 4.5 to evaluate its practical impact.

4 Experimental Results

This section evaluates the effectiveness of the proposed interconnect-aware resynthesis method, ResynMD, from both logic-level and physical design perspectives. We first assess the capability of ResynMD to reduce inter-die connectivity on purely combinational benchmarks, isolating the impact of logic resynthesis without interference from physical design effects. We then study the sensitivity of the proposed approach to LUT size, which directly influences resubstitution opportunities and optimization effectiveness. Finally, we evaluate the downstream impact of interconnect-aware resynthesis on partitioning-based multi-die placement, including wirelength, load balance, and runtime, using realistic heterogeneous FPGA benchmarks.

4.1 Experimental Setup

Our interconnect-aware logic resynthesis method for multi-die FPGAs, ResynMD, is implemented in C++ and Java. All experiments are conducted on a workstation equipped with an AMD Ryzen 9 7900X 12-core processor and 128 GB RAM, running a 64-bit Linux system. For the logic synthesis and technology mapping stage in Figure 4, we use the Yosys [29] and ABC [30] tools. For the partitioning stage, we utilize an hMETIS-based [31] timing-aware partitioning tool. For the physical implementation stage, we utilize the AAPack [32] clustering algorithm provided in VTR8 [33], and the multi-die placement algorithm implemented in LiquidMD [14, 20]. No post-routing results are reported in this work, while our tool flow can be extended to evaluate routing performance in future work.

We fix the imbalance factor UB of the partitioner to 1.25 across all experiments. We evaluate our approach using three benchmark suites, each targeting a distinct evaluation objective. The EPFL [34] benchmark suite consists of purely combinational designs and is used to quantify the intrinsic effectiveness of the proposed logic-level resynthesis in reducing inter-die connections. Since these circuits are relatively small and do not reflect realistic physical-design constraints, we report only connectivity-level metrics on EPFL benchmarks.

To evaluate physical-design impact in the presence of sequential logic, we additionally use a set of MCNC [35] benchmarks. These circuits contain flip-flops but no heterogeneous hard blocks, which enables isolating the effect of sequential elements while still allowing post-placement evaluation.

To evaluate physical-design impact on realistic heterogeneous FPGA designs, we utilize the Koios [36] benchmark suite, which comprises designs featuring hard blocks such as DSPs and block RAMs. In these circuits, hard macros and timing-optimized sequential elements are preserved and

treated as structural boundaries, allowing us to assess whether SLL-aware resynthesis remains beneficial under constrained rewriting flexibility. For both MCNC and Koios, we report post-placement results to quantify downstream physical-design effects.

4.2 Multi-Die Cost Modeling and Connectivity Metrics

During placement, wirelength is commonly estimated by summing the contributions of all nets, where the wirelength of each net is approximated using the half-perimeter wirelength (HPWL) of its bounding box. To account for net-specific characteristics, the HPWL of each net is multiplied by a weighting factor $q(n)$ [14, 20]. The overall wirelength cost is thus defined as

$$BBox_{cost}^{SD} = \sum_{n \in \text{nets}} q(n) \cdot \text{HPWL}(n). \quad (7)$$

for a single-die FPGA.

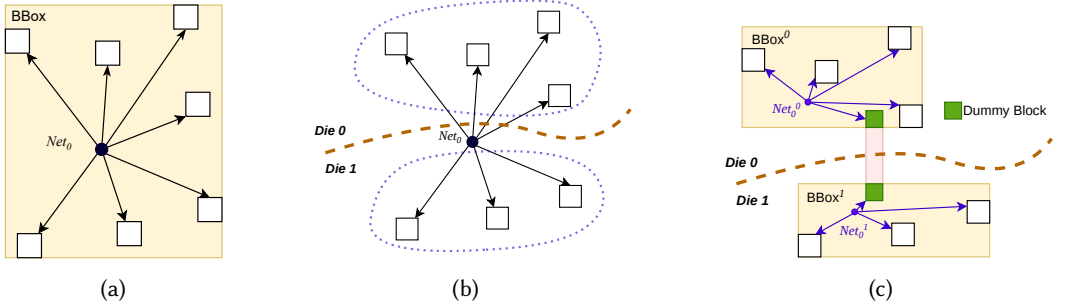


Fig. 7. Bounding-box (BB) wirelength estimation before and after die partitioning [19]. (a) A non-partitioned net enclosed by a single bounding box within one die. (b) After partitioning, the net spans multiple dies, forming die-local terminal clusters. (c) The partitioned net is modeled using multiple die-local bounding boxes connected by inter-die segments, and the total BB wirelength accounts for both intra-die and inter-die components.

For multi-die FPGA systems, Figure 7 illustrates how bounding-box wirelength estimation changes before and after die partitioning. For a non-partitioned design, all terminals of a net are enclosed by a single bounding box within one die (Figure 7a). After partitioning, where partitions equate to dies—nets are classified as intra-die (terminals within one die) or inter-die (crossing boundaries). Intra-die nets use standard HPWL within the die region. For inter-die nets, a single bounding box underestimates wirelength due to long interposer links. Thus, each net is decomposed into die-local segments (evaluated via HPWL with virtual boundary terminals) and an interposer segment modeled as a fixed-length SLL.

Accordingly, the total estimated wirelength of the multi-die system is computed as the sum of the per-die bounding-box costs defined in Equation (7), together with the contribution of inter-die connections, and is expressed as

$$BBox_{cost}^{MD} = \sum_{d \in \mathcal{D}} BBox_{cost}^d + N_{sll} \cdot L_{sll}, \quad (8)$$

where N_{sll} denotes the number of nets crossing the die boundary and L_{sll} is the length of a single interposer link. This modular formulation enables independent optimization of each die during placement while accurately accounting for the cost of timing-expensive inter-die connections.

4.2.1 Multi-Pin Inter-Die Nets and Edge-Level Objective. For a multi-pin net whose sinks are distributed across different dies, current physical design flows typically introduce dummy blocks (e.g., SLL buffers) to model inter-die connections. These dummy blocks are placed at the source and sink sides of the SLLs, enabling consistent modeling in both tile-based and routing-based multi-die FPGA architectures. Furthermore, these cross-die sinks can share the same SLL channel, thereby reducing the second term of the system bounding-box cost in Equation 8.

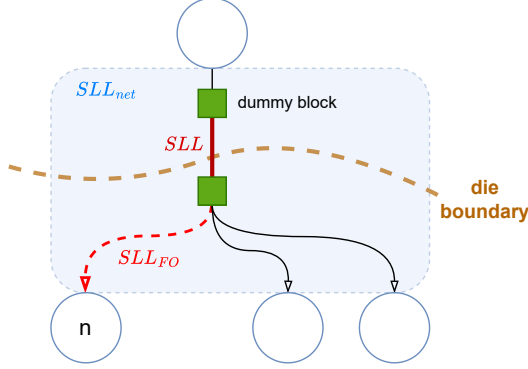


Fig. 8. Illustration of a multi-pin inter-die net implemented via SLL dummy blocks. Eliminating the dependency on node n removes one inter-die connection (i.e., reduces the SLL net’s fanout by one), while the SLL net itself remains due to other cross-die sinks.

As illustrated in Figure 8, in this example, an inter-die net may fan out to multiple sinks on the destination die through an SLL modeled as a dummy block. Each successful resubstitution in resynthesis is *pivot-centric*: the optimization is performed with respect to a selected pivot node, and only its fanin structure is modified. Consequently, the resub removes at most the inter-die fanin edges incident to that pivot, while leaving the fanout structure of the source net unchanged. As illustrated in Figure 8, when node n is selected as the pivot, resubstitution can eliminate its dependency on the inter-die signal, other sinks of the same net remain unaffected. Therefore, a single resubstitution reduces exactly one SLL net’s fanout (SLL_{FO}), but does not eliminate the entire SLL net if additional cross-die sinks still exist. Therefore, inter-die connectivity (N_{Sll}) after physical design implementation does not fully capture the structural impact of SLL-aware resynthesis. For this reason, we refine the definition of inter-die connectivity, using two metrics: the net-level count N_{Sll} and the edge (connection)-level SLL fanout count N_{Sll}^{FO} .

The N_{Sll} counts the number of SLL nets occupying SLL tracks after physical implementation, where multiple cross-die sinks may share the same SLL channel. In contrast, N_{Sll}^{FO} counts each inter-die fanout edge in the LUT-level netlist individually. Each accepted resubstitution guarantees the removal of at least one inter-die edge, strictly reducing N_{Sll}^{FO} even if N_{Sll} remains unchanged.

In what follows, we evaluate the effectiveness of ResynMD on inter-die connectivity in Section 4.3 and its impact on physical design in Section 4.5.

4.3 Impact on Inter-Die Connectivity

We evaluate the effectiveness of ResynMD on pure combinational logic benchmarks from the EPFL benchmark suite. The input netlists are first partitioned using KaHyPar [37] with equal node weights, without considering timing criticality. Subsequently, Algorithm 1 is applied to perform interconnect-aware logic resynthesis. As illustrated in Figure 9, the inter-die connectivity before

and after interconnect-aware resynthesis highlights the effectiveness of the proposed optimization, where plenty of inter-die connections (shown in red) are eliminated.

Tables 3 and 4 summarize the impact of resynthesis on inter-die connectivity and partition balance under both 2-die and 3-die configurations. Across the evaluated benchmarks, ResynMD reduces the number of inter-die connections in a substantial fraction of cases (11/20 for 2-die and 12/20 for 3-die), while leaving others unchanged, which reflects the circuit-dependent nature of resubstitution opportunities.

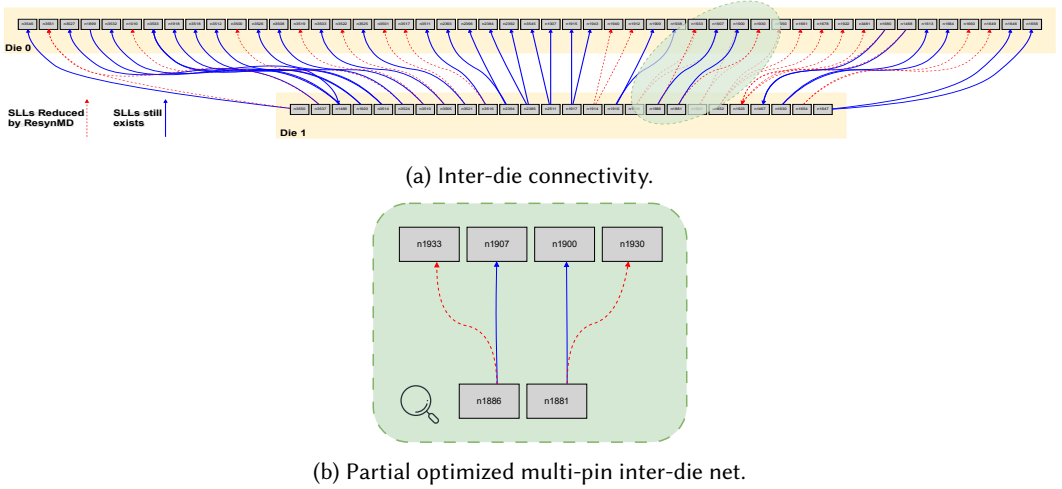


Fig. 9. Inter-die connectivity of a two-die system for the *voter* benchmark from the EPFL suite. Logic blocks are grouped by die. Solid blue edges indicate inter-die connections that remain after resynthesis, while dashed red edges denote inter-die connections eliminated by interconnect-aware resynthesis.

Table 3. Inter-die connections (N_{sll}) and imbalance factor ρ before and after ResynMD on EPFL benchmarks (2-die configuration).

Bench.	N_{sll}				ρ			
	Pre	Resyn	Δ	$\Delta(\%)$	Pre	Resyn	Δ	$\Delta(\%)$
cavlc	42	41	-1	-2.38	1.0070	1.0277	+0.0207	+2.05
arbiter	5430	5171	-259	-4.77	1.0007	1.0000	-0.0007	-0.07
voter	57	32	-25	-43.86	1.0380	1.0010	-0.0370	-3.57
mem_ctrl	1136	815	-321	-28.26	1.0147	1.0161	+0.0014	+0.14
bar	526	458	-68	-12.93	1.0052	1.0084	+0.0032	+0.32
sin	321	248	-73	-22.74	1.0161	1.0650	+0.0489	+4.81
max	213	211	-2	-0.94	1.0374	1.0209	-0.0165	-1.59
square	57	39	-18	-31.58	1.0194	1.0354	+0.0160	+1.56
mult	1000	919	-81	-8.10	1.0003	1.0386	+0.0383	+3.83
log2	3032	1554	-1478	-48.74	1.0328	1.1083	+0.0755	+7.31
hyp	851	279	-572	-67.21	1.0252	1.0221	-0.0031	-0.30
int2float	11	11	0	0	1.0698	1.0698	0	0
Avg.	-	-	-263.45	-24.80	-	-	+0.0133	+1.33

Table 4. Inter-die connections (N_{sll}) and imbalance factor ρ before and after ResynMD on EPFL benchmarks (3-die configuration).

Bench.	N_{sll}				ρ			
	Pre	Resyn	Δ	$\Delta(\%)$	Pre	Resyn	Δ	$\Delta(\%)$
cavlc	61	56	-5	-8.20	1.0385	1.0316	-0.0068	-0.66
arbiter	6322	6259	-63	-1.00	1.0042	1.0047	+0.0005	+0.05
voter	81	41	-40	-49.38	1.0435	1.1038	+0.0604	+5.79
mem_ctrl	2233	1807	-426	-19.09	1.0770	1.0800	+0.0030	+0.28
bar	816	671	-145	-17.77	1.0675	1.0967	+0.0293	+2.74
sin	1412	1123	-289	-20.48	1.0426	1.2183	+0.1758	+16.86
max	311	296	-15	-4.82	1.0187	1.0330	+0.0143	+1.40
square	78	60	-18	-23.08	1.0345	1.0241	-0.0104	-1.00
mult	1846	1704	-142	-7.69	1.0021	1.0721	+0.0700	+6.98
log2	6930	3146	-3784	-54.61	1.0299	1.0591	+0.0292	+2.83
hyp	1276	395	-881	-69.04	1.0253	1.0303	+0.0050	+0.49
int2float	20	19	-1	-5.00	1.1163	1.1163	0.0000	0.00
Avg.	-	-	-467.33	-27.38	-	-	+0.0251	+2.35

Benchmarks with large combinational cones and extensive logic sharing benefit the most, achieving reductions of up to 67.21% for 2-die (69.04% for 3-die) in inter-die connections. On average, interconnect-aware resynthesis reduces inter-die connectivity by 24.80% in the 2-die configuration and by 27.38% in the 3-die configuration. Even if the number of dies increases, each partition becomes smaller, which will reduce the availability of candidate divisors. But at the same time, the total number of inter-die connections increases, creating more opportunities for eliminating logically unnecessary inter-die nets. As a result, the net reduction in N_{sll} is slightly larger in the 3-die case.

The increased effectiveness is likely accompanied by a larger variation in partition imbalance. Compared to the 2-die case, the 3-die configuration exhibits a higher average increase in imbalance ratio calculated from Equation 6 (2.35% versus 1.33%), reflecting the more extensive structural changes introduced by resynthesis. Nevertheless, all observed imbalance values remain within practical bounds, and stricter imbalance constraints can be imposed during the initial partitioning stage if needed. Figure 10 further illustrates the relationship between inter-die connectivity reduction and imbalance variation. No strong correlation is observed between $\Delta\rho$ and ΔN_{sll} , and several circuits achieve substantial SLL reduction with negligible imbalance change. This suggests that the effectiveness of ResynMD does not inherently rely on increasing partition imbalance.

4.3.1 Physical Implications of Edge-Level SLL Reduction. Although ResynMD does not always reduce the number of SLL nets (N_{sll}), it consistently reduces the number of inter-die connections (N_{sll}^{FO}). This distinction is important from a physical design perspective. As illustrated by the green zoomed-in nets in Figure 9b, one inter-die connection is removed, while another remains. High-fanout inter-die nets impose disproportionate routing and timing pressure, as they load inter-die resources and near-die boundary routing resources, and increase routing complexity within the destination die.

Reducing the number of inter-die SLL fanouts (N_{sll}^{FO}) decreases SLL loading and mitigates routing congestion around SLL endpoints. Since SLL sink locations are fixed at the die boundary and already incur substantial inter-die delay, signals traversing SLLs typically exhibit high arrival times and timing criticality. Under congestion, routing detours near these fixed interface points can further increase delay and exacerbate timing violations. By reducing inter-die fanout, the proposed method

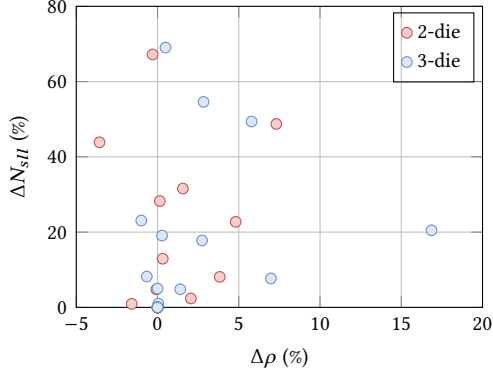


Fig. 10. Trade-off between inter-die connectivity reduction and imbalance variation under 2-die and 3-die configurations.

alleviates local congestion pressure around SLL interfaces, thereby improving routability and timing robustness even when the total number of occupied SLL tracks remains unchanged.

4.4 Impact of LUT Size on SLL-Aware Resynthesis Effectiveness

The effectiveness of SLL-aware resynthesis is strongly influenced by the target LUT size, which directly determines structural flexibility and divisor availability in the mapped LUT-level netlist. Smaller LUT sizes produce finer-grained logic decomposition, resulting in a larger number of nodes with simpler Boolean functions. This increases the number of candidate divisors within each resubstitution window and reduces SAT constraint complexity, thereby improving the likelihood of finding valid in-die replacements. In contrast, larger LUT sizes consolidate logic into fewer nodes with higher functional complexity. This reduces the available divisor set and enlarges the SAT search space, making it more difficult to identify feasible substitutions that reduce inter-die connectivity.

To quantify this sensitivity, we map the EPFL benchmarks to LUT-4/5/6 and measure the reduction in inter-die SLL nets after resubstitution, as summarized in Table 5. In this experiment, we use a larger window size than in the previous effectiveness study to avoid overly restricting the divisor space. Unlike the previous experiments that use min-cut partitioners (KaHyPar/hMetis), the initial die assignment here is generated by a deterministic hash-based labeling scheme to eliminate partitioning variability across different LUT mappings. Since this pseudo-partition is not optimized for cut minimization, the initial inter-die connectivity is typically higher, providing more opportunities for resubstitution to remove cross-die nets. As a result, the absolute SLL reductions are larger than those in Section 4.3, but still adequate for comparing LUT-size impact.

On average, LUT4 achieves the largest reduction (2243.42 nets), followed by LUT5 (1838.26), while LUT6 shows the smallest improvement (1622.11). This trend is consistent across most benchmarks, indicating that LUT granularity plays a critical role in interconnect-aware optimization. Post-partition resubstitution benefits from finer-grained logic representations, while larger LUT sizes limit optimization opportunities due to reduced structural flexibility.

4.5 Impact on Physical Design (Placement)

The target chip is configured as a 325×436 -tile FPGA, partitioned into a 2×1 multi-die layout. Each die spans 325×218 tiles. The two dies are interconnected through 36 rows of super-long lines, each

Table 5. Reduction in inter-die SLL edges ΔN_{sll} under different LUT sizes (LUT-4/5/6).

Bench.	LUT4	LUT5	LUT6	Bench.	LUT4	LUT5	LUT6
int2float	46	33	25	sin	1382	1259	1155
ctrl	23	6	5	max	568	477	388
router	37	30	30	square	3789	3351	2949
cavlc	179	115	53	sqrt	3255	3205	2660
priority	145	113	105	multiplier	5107	4795	4328
dec	32	31	31	log2	6889	6141	5610
i2c	177	129	104	div	4538	3290	4032
arbiter	2215	1729	1417	voter	1960	1772	1425
mem_ctrl	9361	7374	6077				
Total	42625	34927	30820	Average	2243.42	1838.26	1622.11

modeled with a fixed delay of 2.224 ns. We first evaluate the effectiveness of the proposed method on the MCNC benchmarks and assess its impact on physical design using sequential circuits. We then extend the study to designs containing hard blocks from the Koios benchmark suite.

4.5.1 Inter-Die Connectivity Reduction. Table 6 reports the impact of ResynMD on inter-die connectivity under the 2-die configuration. Across the MCNC [35] benchmarks, the proposed method reduces inter-die fanout edges by 12.29% on average, while the net-level reduction is 1.65%. The discrepancy between edge-level and net-level improvements is expected. Multiple cross-die sinks may share a single SLL track, and removing individual fanout edges does not necessarily eliminate the occupied SLL channel. Nevertheless, reducing inter-die fanout edges lowers SLL loading and simplifies inter-die connectivity at the structural level.

4.5.2 Placement Quality and Load Balance. The reduction in inter-die connectivity translates to modest improvements in placement quality. On MCNC benchmarks, the average bounding-box cost decreases by 1.13%. Although the average BBox reduction appears modest, it reflects a more spatially compact placement solution. Reducing inter-die fanout edges shortens the effective span of inter-die nets, which decreases routing demand and alleviates congestion in multi-die architectures. Circuits exhibiting larger edge-level reductions (e.g., *ex5p* and *pdc*) show more noticeable BBox improvements, suggesting that reduced inter-die coupling can alleviate global placement pressure. These effects are expected to become more pronounced during routing, as reduced congestion could potentially lower the number of rip-up-and-reroute iterations. A detailed routing-level analysis is left for future work.

Die-level load balance remains largely stable. The pre-pack imbalance factor changes by -0.40% on average, while the post-pack imbalance varies by $+0.37\%$. These small variations indicate that interconnect-aware resynthesis does not significantly distort partition balance and remains compatible with partitioning-based multi-die flows. The imbalance change at the LUT-level is smaller than the intrinsic variation introduced by the packing stage. Placement runtime is also stable, with an average change of -0.44% , demonstrating that the proposed method does not introduce additional overhead in the physical design stage.

In cases of partition imbalance, the optimization can be restricted to nodes in the smaller die subgraph, potentially reducing the effective size of the larger die and improving partition balance. Since the optimization objective adheres to the area constraint defined in Equation 2, the total circuit size is guaranteed to be non-increasing, with only a possible increase in edge count due to additional fanout connections of selected divisors. Therefore, even if the imbalance factor slightly

Table 6. Impact of ResynMD on inter-die connectivity, placement quality, load balance, and placement runtime across MCNC benchmarks.

Bench.	N_{sil}			$N_{\text{sil}}^{\text{FO}}$			$B\text{Box}_{\text{cost}}^{\text{2die}}$			ρ_{pre}			ρ_{post}			Runtime _{place}		
	P	R	Δ	P	R	Δ	P	R	Δ	P	R	Δ	P	R	Δ	P	R	Δ
apex2	66	64	-2	400	293	-107	582.9	575.3	-7.6	1.130	1.129	-0.0005	1.128	1.123	-0.005	0.580	0.564	-0.016
apex4	134	134	0	872	827	-45	601.8	594.5	-7.3	1.151	1.146	-0.005	1.131	1.138	+0.007	0.517	0.522	+0.005
bigkey	6	6	0	784	784	0	459.9	424.8	-35.1	1.006	1.006	0.000	1.000	1.000	0.000	0.644	0.651	+0.006
clma	143	141	-2	3821	2879	-942	1996.4	2017.8	+21.4	1.142	1.135	-0.007	1.141	1.142	+0.002	0.791	0.791	0.000
des	11	11	0	581	581	0	325.0	346.3	+21.3	1.026	1.026	0.000	1.025	1.024	-0.0002	0.723	0.706	-0.018
diffeq	49	49	0	995	980	-15	468.0	465.8	-2.2	1.130	1.130	0.000	1.128	1.134	+0.006	0.545	0.539	-0.006
dsip	3	3	0	560	560	0	281.0	275.5	-5.4	1.008	1.008	0.000	1.006	1.006	0.000	0.624	0.627	+0.003
ex5p	186	165	-21	922	679	-243	758.3	673.8	-84.5	1.167	1.145	-0.022	1.155	1.126	-0.029	0.559	0.538	-0.021
frisc	173	173	0	3075	2772	-303	1142.8	1127.8	-15.0	1.064	1.064	0.000	1.054	1.052	-0.002	0.639	0.633	-0.006
misex3	117	116	-1	806	693	-113	596.3	595.9	-0.4	1.157	1.144	-0.013	1.148	1.149	+0.002	0.536	0.533	-0.003
pdc	312	303	-9	5577	4547	-1030	1469.9	1411.7	-58.2	1.171	1.155	-0.015	1.152	1.186	+0.033	0.644	0.661	+0.017
s38417	46	46	0	2276	2204	-72	1047.1	1070.6	+23.5	1.001	1.001	0.000	1.000	1.003	+0.003	0.724	0.717	-0.007
s38584.1	21	21	0	479	471	-8	1110.2	1158.2	+48.1	1.106	1.106	0.000	1.082	1.088	+0.006	0.737	0.753	+0.016
seq	112	111	-1	671	560	-111	732.0	768.8	+36.8	1.130	1.125	-0.005	1.126	1.128	+0.002	0.596	0.599	+0.003
tseng	35	35	0	636	628	-8	478.0	472.2	-5.9	1.150	1.151	+0.001	1.072	1.107	+0.035	0.590	0.577	-0.013
Avg.	-	-	-2.40	-	-	-199.7	-	-	-4.69	-	-0.0044	-	-	+0.0040	-	-	-	-0.0027

-0.44

Table 7. Impact of ResynMD on timing cost (total arrival time) and critical-path delay (CPD) across MCNC benchmarks, both reported in *ns*.

Bench.	Timing cost (<i>ns</i>)				CPD (<i>ns</i>)			
	Prev	Resynsn	Δ	%	Prev	Resynsn	Δ	%
apex2	6267.0	6094.5	-173.0	-2.75	42.71	31.16	-11.56	-27.06
apex4	2928.4	2768.9	-159.0	-5.45	42.25	38.42	-3.83	-9.07
bigkey	4285.2	4045.5	-240.0	-5.59	33.75	33.98	+0.23	+0.68
clma	9243.5	10042.0	+799.0	+8.64	34.64	39.41	+4.77	+13.77
des	2896.7	3112.3	+216.0	+7.45	36.37	34.69	-1.67	-4.60
diffeq	1356.4	1183.9	-173.0	-12.72	38.24	31.10	-7.14	-18.68
dsip	2406.0	2386.3	-19.7	-0.82	31.40	27.27	-4.13	-13.15
ex5p	3002.3	2553.5	-449.0	-14.95	46.00	39.55	-6.44	-14.01
frisc	4429.4	4210.9	-219.0	-4.93	33.93	45.84	+11.92	+35.12
misex3	5070.9	5662.7	+592.0	+11.67	36.25	29.44	-6.81	-18.78
pdc	7935.8	7214.6	-721.0	-9.09	43.67	44.07	+0.41	+0.93
s38417	2872.2	2954.1	+81.9	+2.85	29.21	24.77	-4.43	-15.18
s38584.1	2018.8	1852.1	-167.0	-8.25	30.74	30.54	-0.20	-0.64
seq	5001.5	6685.2	+1680.0	+33.66	34.36	38.20	+3.83	+11.15
tseng	918.5	921.8	+3.3	+0.36	28.04	26.98	-1.06	-3.76
Avg.	-	-	+70.10	+0.01	-	-	-1.74	-4.22

Table 8. Impact of ResynMD on physical design across Koios benchmarks with reduced inter-die connectivity (2-die configuration).

Bench.	Inter-die connectivity		Post-placement metrics			
	ΔN_{sll}	$\Delta N_{\text{sll}}^{FO}$	$\Delta BBox_{\text{cost}}^{2\text{die}}$ (%)	Δ Timing (%)	Δ CPD (%)	Δ Runtime (%)
robot_rl	0 (0.00%)	-189 (-10.79%)	-2.18	+5.77 \uparrow	+0.42	-0.88
tpu_like.medium	-2 (-0.61%)	-980 (-2.68%)	-7.25 \downarrow	+3.85	+5.80 \uparrow	+0.74
lstm	0 (0.00%)	-145 (-0.25%)	-8.89 \downarrow	-5.50 \downarrow	-2.71	-1.35
reduction_layer	0 (0.00%)	-8 (-0.10%)	-0.17	+4.86	-20.23 \downarrow	-2.04
softmax	0 (0.00%)	-4 (-0.24%)	-2.68	+1.02	-21.42 \downarrow	-1.22
dla_like.medium	0 (0.00%)	-1 (-0.00%)	+1.80	+7.15 \uparrow	-1.08	-2.69
dla_like.small	0 (0.00%)	-7 (-0.01%)	+0.13	+21.92 \uparrow	-1.54	-2.70

*Arrows indicate significant variations ($|\Delta| > 5\%$).

increases (e.g., due to further reduction of the smaller die), the downstream physical design stages are not adversely affected compared with the baseline flow.

4.5.3 Timing Behavior. The impact on timing is circuit-dependent, as shown in Table 7. While several benchmarks (e.g., *ex5p*, *diffeq*, and *pdc*) exhibit timing improvement, some of the others experience degradation. On average, the critical-path delay (CPD) decreases by -4.22% . This non-uniform behavior is attributed to the absence of explicit timing constraints in the resynthesis objective. While minimizing inter-die fanout effectively alleviates routing congestion and SLL overhead, logic resubstitution carries the risk of selecting timing-critical signals as divisors for node interpolation. The example in Figure 6b illustrates this issue, although the SLL at the pivot node is eliminated, the selected divisor Y lies on a timing-critical path, and its own fanin already crosses die boundaries. This process inadvertently extends the critical path and sabotages timing slack. Therefore, inter-die connectivity reduction alone does not guarantee timing improvement. Incorporating slack-based information as the cost function of SLL-aware logic resynthesis can prevent

timing degradation; however, this comes at the expense of resubstitution efficacy. These observations highlight the complex interaction between logic-level restructuring and downstream multi-die placement optimization.

4.5.4 Heterogeneous Koios Benchmarks. As shown in Table 8, in Koios benchmarks that contain hard blocks, net-level SLL reductions ΔN_{sll} are limited, and edge-level improvements ΔN_{sll}^{FO} are generally small. This is expected, as inter-die connectivity in heterogeneous designs is often dominated by hard macros that cannot be modified by LUT-level resubstitution. In the current Koios flow, the circuits are technology-mapped and timing-optimized prior to resynthesis. Hard blocks and sequential latches are treated as black boxes, and their I/Os are exposed to the LUT-level netlist as primary inputs and outputs. As a result, logical continuity across these modules is structurally interrupted. During window-based resubstitution, such boundaries restrict the availability of valid divisors, since signals cannot propagate across black-box interfaces.

Nevertheless, due to computational resource constraints, we conducted full physical design experiments on 15 Koios circuits, among which 8 exhibit measurable reductions in inter-die connectivity under ResynMD. certain designs such as *lstm* and *tpu_like.medium* exhibit BBox reductions of up to 8.89% and 7.25% respectively, with an average of 2.75% reduction on 7 listed circuits. Although net-level SLL reduction is limited in heterogeneous circuits dominated by hard macros, these results indicate that even modest edge-level improvements within combinational regions can reshape spatial placement organization. In terms of timing, the average CPD across the seven listed Koios benchmarks decreases by 5.82%, although the behavior remains design-dependent. Significant improvements are observed in designs such as *reduction_layer* and *softmax*, where CPD decreases by over 20%. These results suggest that even when net-level SLL reduction is structurally constrained, localized edge-level simplification can still mitigate inter-die routing overhead and reduce critical-path sensitivity to SLL delay.

These observations imply that SLL-aware resynthesis would be more effective if applied before hard-block binding and physical synthesis. Performing logic restructuring earlier in the flow would provide greater structural freedom and potentially expose more opportunities for reducing inter-die connectivity.

5 Conclusion and Future Work

This paper presents ResynMD, an interconnect-aware logic resynthesis method integrated into a partitioning-based multi-die tool flow to reduce inter-die connections. To the best of our knowledge, this is the first work to incorporate logic resynthesis into a multi-die FPGA CAD flow for inter-die connection optimization. By targeting LUT-level logic that contributes substantially to inter-die connections, ResynMD is orthogonal to existing partitioning-based flows and demonstrates that logic resynthesis can reduce inter-die connections that partitioning alone cannot eliminate. Experimental results show that ResynMD reduces inter-die connections across a wide range of benchmarks, with particularly strong benefits for combinational and soft-logic-dominated designs. These improvements are achieved while maintaining acceptable partition balance and successful physical implementation. The reduction in inter-die connections also leads to downstream effects on physical metrics after placement, such as wirelength and critical path delay.

Future work will incorporate routing into both the evaluation and the resynthesis objective, enabling a more realistic assessment of inter-die routing resource usage and overall implementation quality. Finally, although this work focuses on LUT-based FPGA fabrics, the principle of interconnect-aware logic resynthesis can be extended to chiplet-based ASIC systems or 3D ICs, where inter-die or inter-layer interconnects similarly incur high delay and routing cost. In such settings, the optimization would operate on technology-mapped gate-level netlist rather than on LUT-level

netlists, by performing functionality-preserving transformations to reduce inter-die or inter-layer connections.

References

- [1] Riko Radojčić. *More-than-Moore 2.5 D and 3D SiP integration*. Springer, 2017.
- [2] Alexander Graening, Puneet Gupta, Andrew B. Kahng, Bodhisatta Pramanik, and Zhiang Wang. ChipletPart: Cost-aware partitioning for 2.5D systems, 2025.
- [3] Andre Hahn Pereira and Vaughn Betz. CAD and routing architecture for interposer-based multi-FPGA systems. In *Proceedings of the 2014 ACM/SIGDA International Symposium on Field-Programmable Gate Arrays*, FPGA '14, page 75–84, New York, NY, USA, 2014. Association for Computing Machinery.
- [4] Andrew Boutros, Fatemehsadat Mahmoudi, Amin Mohaghegh, Stephen More, and Vaughn Betz. Into the third dimension: Architecture exploration tools for 3D reconfigurable acceleration devices. In *2023 International Conference on Field Programmable Technology (ICFPT)*, pages 198–208. IEEE, 2023.
- [5] Ehsan Nasiri, Javeed Shaikh, Andre Hahn Pereira, and Vaughn Betz. Multiple dice working as one: CAD flows and routing architectures for silicon interposer FPGAs. *IEEE Transactions on Very Large Scale Integration (VLSI) Systems*, 24(5):1821–1834, 2016.
- [6] Xiaoke Wang and Dirk Stroobandt. The influence of interconnection complexity on the FPGA CAD flow. In *Proceedings of the 2024 ACM International Workshop on System-Level Interconnect Pathfinding*, SLIP '24, New York, NY, USA, 2025. Association for Computing Machinery.
- [7] Zhixiong Di, Runzhe Tao, Jing Mai, Lin Chen, and Yibo Lin. LEAPS: Topological-layout-adaptable multi-die FPGA placement for super long line minimization. *IEEE Transactions on Circuits and Systems I: Regular Papers*, 71(3):1259–1272, 2024.
- [8] Licheng Guo, Yuze Chi, Jie Wang, Jason Lau, Weikang Qiao, Ecenur Ustun, Zhiru Zhang, and Jason Cong. Autobridge: Coupling coarse-grained floorplanning and pipelining for high-frequency hls design on multi-die FPGAs. In *The 2021 ACM/SIGDA International Symposium on Field-Programmable Gate Arrays*, FPGA '21, page 81–92, New York, NY, USA, 2021. Association for Computing Machinery.
- [9] Linfeng Du, Tingyuan Liang, Sharad Sinha, Zhiyao Xie, and Wei Zhang. FADO: Floorplan-aware directive optimization for high-level synthesis designs on multi-die FPGAs. In *Proceedings of the 2023 ACM/SIGDA International Symposium on Field Programmable Gate Arrays*, FPGA '23, page 15–25, New York, NY, USA, 2023. Association for Computing Machinery.
- [10] Wan-Sin Kuo, Shi-Han Zhang, Wai-Kei Mak, Richard Sun, and Yoon Kah Leow. Pin assignment optimization for multi-2.5 D FPGA-based systems. In *Proceedings of the 2018 International Symposium on Physical Design*, pages 106–113, 2018.
- [11] Yu-Chen Liao and Wai-Kei Mak. Pin assignment optimization for multi-2.5 D FPGA-based systems with time-multiplexed I/Os. *IEEE Transactions on Computer-Aided Design of Integrated Circuits and Systems*, 40(3):494–506, 2020.
- [12] Jason Luu, Jeffrey Goeders, Michael Wainberg, Andrew Somerville, Thien Yu, Konstantin Nasartschuk, Miad Nasr, Sen Wang, Tim Liu, Nooruddin Ahmed, Kenneth B. Kent, Jason Anderson, Jonathan Rose, and Vaughn Betz. VTR 7.0: Next generation architecture and CAD system for FPGAs. *ACM Trans. Reconfigurable Technol. Syst.*, 7(2), July 2014.
- [13] Mahesh A. Iyer, Andrew B. Kahng, Jason Luu, Bodhisatta Pramanik, Kristofer Vorwerk, and Grace Zgheib. A Partitioning-Based CAD Flow for Interposer-Based Multi-Die FPGAs. In *2025 IEEE 33rd Annual International Symposium on Field-Programmable Custom Computing Machines (FCCM)*, pages 172–180, May 2025. ISSN: 2576-2621.
- [14] Raveena Raikar and Dirk Stroobandt. LiquidMD: Optimizing inter-die and intra-die placement for 2.5D FPGA architectures. In *Proceedings of the 14th International Symposium on Highly Efficient Accelerators and Reconfigurable Technologies*, HEART '24, page 90–98, New York, NY, USA, 2024. Association for Computing Machinery.
- [15] AMD Xilinx. Alveo U200 and U250 data center accelerator cards, 2023.
- [16] Chirag Ravishankar, Henri Fraise, and Dinesh Gaitonde. SAT based place-and-route for high-speed designs on 2.5D FPGAs. In *2018 International Conference on Field-Programmable Technology (FPT)*, pages 118–125. IEEE, 2018.
- [17] Oleg Petelin and Vaughn Betz. The speed of diversity: Exploring complex FPGA routing topologies for the global metal layer. In *2016 26th International Conference on Field Programmable Logic and Applications (FPL)*, pages 1–10, 2016.
- [18] Xibo Sun, Hao Zhou, and Lingli Wang. Bent routing pattern for FPGA. In *2019 29th International Conference on Field Programmable Logic and Applications (FPL)*, pages 9–16, 2019.
- [19] Raveena Raikar and Dirk Stroobandt. Multi-die heterogeneous FPGAs: How balanced should netlist partitioning be? In *Proceedings of the 24th ACM/IEEE Workshop on System Level Interconnect Pathfinding*, SLIP '22, New York, NY, USA, 2023. Association for Computing Machinery.
- [20] Dries Verucryce, Elias Vansteenkiste, and Dirk Stroobandt. Liquid: High quality scalable placement for large heterogeneous FPGAs. In *2017 International Conference on Field Programmable Technology (ICFPT)*, pages 17–24, 2017.
- [21] Dries Verucryce, Elias Vansteenkiste, and Dirk Stroobandt. How preserving circuit design hierarchy during FPGA packing leads to better performance. *IEEE Transactions on Computer-Aided Design of Integrated Circuits and Systems*, 37(3):629–642, 2018.

- [22] Alan Mishchenko and Robert Brayton. Scalable logic synthesis using a simple circuit structure. In *International Workshop on Logic Synthesis*, volume 6, pages 15–22, 2006.
- [23] Siang-Yun Lee et al. A simulation-guided paradigm for logic synthesis and verification. *IEEE Transactions on Computer-Aided Design of Integrated Circuits and Systems*, 41(8):2573–2586, 2021.
- [24] Luca Amarú, Mathias Soeken, Patrick Vuillot, Jiong Luo, Alan Mishchenko, Janet Olson, Robert Brayton, and Giovanni De Micheli. Improvements to Boolean resynthesis. In *2018 Design, Automation & Test in Europe Conference & Exhibition (DATE)*, pages 755–760. IEEE, 2018.
- [25] Fangzhou Liu et al. CBTune: Contextual bandit tuning for logic synthesis. In *2024 Design, Automation & Test in Europe Conference & Exhibition (DATE)*, 2024.
- [26] Alan Mishchenko, Robert Brayton, Jie-Hong R. Jiang, and Stephen Jang. Scalable don’t-care-based logic optimization and resynthesis. *ACM Trans. Reconfigurable Technol. Syst.*, 4(4), December 2011.
- [27] Alan Mishchenko, Jin S Zhang, Subarnarekha Sinha, Jerry R Burch, Robert Brayton, and Malgorzata Chrzanowska-Jeske. Using simulation and satisfiability to compute flexibilities in boolean networks. *IEEE Transactions on Computer-Aided Design of Integrated Circuits and Systems*, 25(5):743–755, 2006.
- [28] Chih-Chun Lee, Jie-Hong R. Jiang, Chung-Yang Huang, and Alan Mishchenko. Scalable exploration of functional dependency by interpolation and incremental sat solving. In *2007 IEEE/ACM International Conference on Computer-Aided Design*, pages 227–233, 2007.
- [29] Claire Wolf. Yosys Open SYnthesis Suite. <https://yosyshq.net/yosys/>, 2025.
- [30] Robert Brayton and Alan Mishchenko. ABC: An academic industrial-strength verification tool. In *International Conference on Computer Aided Verification*, pages 24–40. Springer, 2010.
- [31] George Karypis and Vipin Kumar. A hypergraph partitioning package. *Army HPC Research Center, Department of Computer Science & Engineering, University of Minnesota*, 1998.
- [32] Jason Luu, Jason Anderson, and Jonathan Rose. Architecture description and packing for logic blocks with hierarchy, modes and complex interconnect. In *Proceedings of the 19th ACM/SIGDA International Symposium on Field Programmable Gate Arrays*, FPGA ’11, page 227–236, New York, NY, USA, 2011. Association for Computing Machinery.
- [33] Kevin E. Murray, Oleg Petelin, Sheng Zhong, Jia Min Wang, Mohamed Eldafrawy, Jean-Philippe Legault, Eugene Sha, Aaron G. Graham, Jean Wu, Matthew J. P. Walker, Hanqing Zeng, Panagiotis Patros, Jason Luu, Kenneth B. Kent, and Vaughn Betz. VTR 8: High-performance CAD and Customizable FPGA Architecture Modelling. *ACM Transactions on Reconfigurable Technology and Systems*, 13(2):1–55, June 2020.
- [34] Luca Amarú, Pierre-Emmanuel Gaillardon, and Giovanni De Micheli. The EPFL combinational benchmark suite. *Hypotenuse*, 256(128):214335, 2015.
- [35] Saeyang Yang. *Logic synthesis and optimization benchmarks user guide: version 3.0*. Microelectronics Center of North Carolina (MCNC) Research Triangle Park, NC, USA, 1991.
- [36] Aman Arora, Andrew Boutros, Daniel Rauch, Aishwarya Rajen, Aatman Borda, Seyed Alireza Damghani, Samidh Mehta, Sangram Kate, Pragnesh Patel, Kenneth B Kent, et al. Koios: A deep learning benchmark suite for FPGA architecture and CAD research. In *2021 31st International Conference on Field-Programmable Logic and Applications (FPL)*, pages 355–362. IEEE, 2021.
- [37] Sebastian Schlag, Tobias Heuer, Lars Gottesbüren, Yaroslav Akhremtsev, Christian Schulz, and Peter Sanders. High-quality hypergraph partitioning. *ACM J. Exp. Algorithmics*, mar 2022.

Received Day Month Year; revised Day Month Year; accepted Day Month Year